Calculations of the ^{6}He+p Elastic Scattering Cross Sections within the Folding Approach and High-energy Approximation for the Optical Potential

E. V. Zemlyanaya[1], V. K. Lukyanov[1], K. V. Lukyanov[1], A. N. Antonov[2], and M. K. Gaidarov[2]

[1] Joint Institute for Nuclear Research, Dubna 141980, Russia
[2] Institute of Nuclear Research and Nuclear Energy, Bulgarian Academy of Sciences, 1784 Sofia, Bulgaria

Abstract. Calculations of microscopic optical potentials (OP's) (the real and imaginary parts) are performed to analyze the ^{6}He+p elastic scattering data at tens of MeV/nucleon (MeV/N). The OP's were constructed on the basis of two microscopic models (the folding procedure and the high-energy approximation) using three model densities of ^{6}He. Cross sections were calculated with a help of DWUCK4 code. The effect on cross sections of the dependence of the NN-forces on nuclear matter density is investigated. The role of the spin-orbital terms and the non-linearity of the OP's and also the role of its renormalization are studied. The sensitivity of the cross sections to these effects is tested.

1 Introduction

The basic characteristics of the exotic nucleus ^{6}He with two neutrons in the far periphery ("halo") have been studied on the basis of analyzes of the experimental data on scattering and reactions. For instance, the measurements of the elastic scattering cross sections at energies less than 100 MeV/N have been performed in [1–10]. Their analysis has been carried out (see, *i.e.* [9–17]) by using phenomenological OP's (with many parameters), as well as using OP's calculated within semi-microscopic approaches. With respect to the latter, actually only the real part of the OP's has been calculated, while the imaginary part is taken in a phenomenological form. For calculations of the OP real part $V^F = V^D + V^{EX}$ the folding model [18–20] has been used, in which the direct $V^D(r)$ and exchange $V^{EX}(r)$ parts have been elaborated separately. Each one of these parts is given by a folding of the density ρ_2 of the ^{6}He nucleus with an effective NN potential $v(s)$. As an example we give here only the direct part of the OP:

$$V^D(r) = g(E) \int d^3r_2 \, \rho_2(\mathbf{r_2}) \, F(\rho_2) \, v_{00}^D(s), \qquad \mathbf{s} = \mathbf{r_2} + \mathbf{r}, \tag{1}$$

where the factor $g(E)$ parametrizes the energy dependence of the potential, while $F(\rho_2)$ gives the in-medium dependence of the NN forces $v_{00}^D(s)$. (The expression for the exchange part of the real OP can be found in [19–21], and the necessary

parameters used are given in [21]). The spin-orbit part of the potential is introduced also phenomenologically as a function with fitting parameters. This semi-microscopic approach has been used in recent papers [15–17], where a conclusion on sensitivity of the calculated cross sections to the choice of the structure model of ^{6}He has been made.

It is of interest to carry out a similar analysis on a fully microscopic basis, where both real and imaginary parts of the OP can be calculated. In principle, there exists a theory of scattering of complex systems, *e.g.* the unified theory of reactions [22], that gives a general recipe for construction of the OP. However, in practice one starts from the conditions of the particular task, taking into account the most important channels of the studied process, *e.g.* the multiple scattering and the transfer of nucleons, the fragmentation and other reactions [23, 24]. It turns out, that at relatively high energies of the nucleon scattering of nuclei (the case of inverse kinematics to the ^{6}He+p scattering) the most successful approach is based on the Glauber-Sitenko theory [25, 26]. In it the multiple scattering of the incident particle on the nuclear nucleons in the nucleus is taken into account. Important ingredients of the theory are the nuclear density distribution function and the NN scattering amplitude. In its optical limit this theory leads to the microscopic eikonal form of the scattering phase where the form factors of the nuclear density profile functions and the NN amplitude are folded. Then, using the definition of the eikonal phase as an integral from the nucleon-nucleus potential over the trajectory of the straight-line propagation, it is possible to obtain an expression for the OP as a folding of the nuclear form factors and the NN amplitude [27, 28]

$$U^H = V^H + iW^H = -\frac{\hbar v}{(2\pi)^2}\,(\bar{\alpha}_{NN}+i)\,\bar{\sigma}_{NN}\int\limits_0^\infty dq\; q^2 j_0(qr)\rho_2(q) f_{NN}(q), \quad (2)$$

where $\bar{\sigma}_{NN}$ and $\bar{\alpha}_{NN}$ are, correspondingly, the averaged over the isospin of the nucleus total NN scattering cross section and the ratio of the real to imaginary parts of the forward NN scattering amplitude, both being parametrized in [29, 30] as functions of the energy.

2 Results of Calculations

The general aim in this work is to study the ability of the microscopically calculated OP's (including also the check of the lowest energy of its applicability) to be used for description of the available data on the differential ^{6}He+p elastic cross sections at energies up to 100 MeV/N. It is important also that the fully microscopic OP does not include free parameters but depends on the density distribution of ^{6}He, and this allows one to test the various existing models of this nucleus. We utilized the ^{6}He densities from the semi-empirical model of Tanihata [31], the cluster-orbital shell-model approach (COSMA) [13] and the large-scale shell model (LSSM) in which a large number of shells is taken into account [32] (see for details [33]). In Figure 1

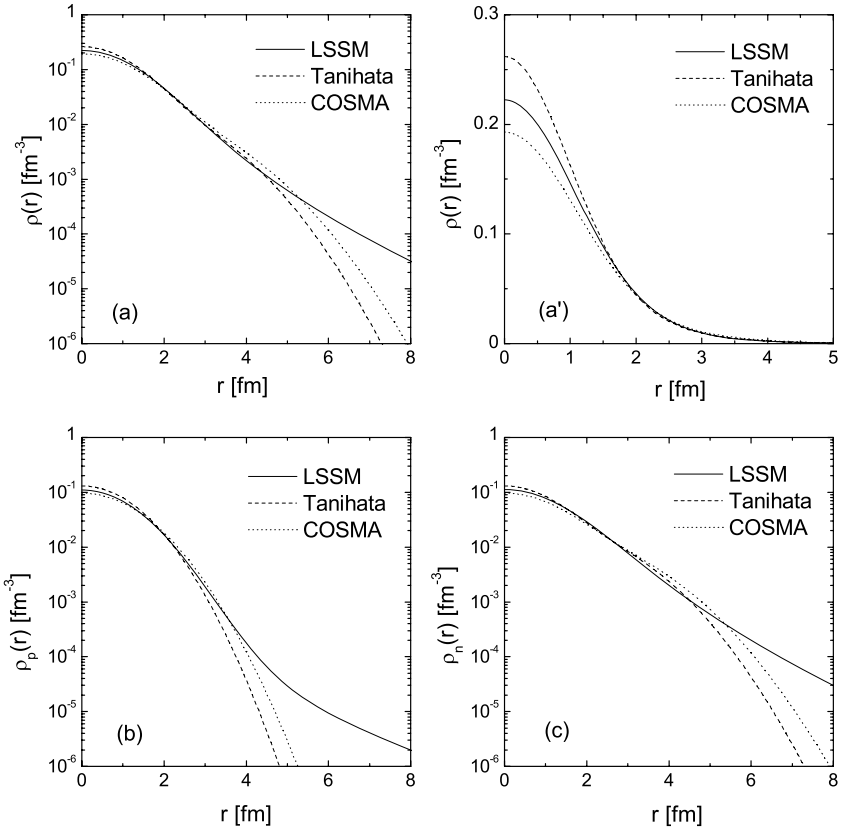

Figure 1. Total ((a) and (a')), proton (b) and neutron (c) densities of ^{6}He calculated in the models of Tanihata *et al.* [31], COSMA [13] and LSSM [32].

are given in logarithmic and linear scale the forms of the proton, neutron and nuclear densities of ^{6}He obtained in these models. Among them only the LSSM density has a realistic exponential behavior at asymptotically large distances, while the others have a Gaussian asymptotics.

On the basis of the microscopically calculated OP's we obtained the differential elastic scattering cross sections using the DWUCK4 code [34]. Three forms of the OP's based on different combinations of the microscopic real and imaginary parts of the OP's have been studied:

$$(A) \qquad U^A_{opt} = N^A_R V^H + iN^A_I W^H, \tag{3}$$

$$(B) \qquad U^B_{opt} = N^B_R V^F + iN^B_I W^H, \tag{4}$$

$$(C) \qquad U^C_{opt} = N^C_R V^F + iN^C_I V^F. \tag{5}$$

Here V^H and W^H are the High-Energy Approximation (HEA) real and imaginary OP's respectively, and V^F is the real OP obtained within the folding approach.

It consists of the direct V^D and the exchange V^{EX} parts. In some cases it became necessary to vary the strength of the parts of the OP's including corresponding fitting coefficients N_R and N_I(no more than two for each part of the OP). The spin-orbit potential was introduced following the standard definition

$$U_{so} \simeq N_{so}\lambda_\pi^2 \left(\frac{1}{r}\right) \frac{df(r)}{dr}, \tag{6}$$

where $f(r)$ is the form of the real part of OP, and λ_π^2=2 fm^2.

The role of the spin-orbit part of OP is shown in Figure 2. The results of the calculations in three cases are presented: a) when $N_{so} = 0.5$ and $f(r)$ is taken to be the microscopically calculated $V^F(r)$ (solid curves); b) $N_{so} = 6.2$ MeV and $f(r)$ has the form of the Woods-Saxon (WS) potential with the fitted form factor from [35] (dashed curves); c) without the spin-orbit term, *i.e.* $N_{so} = 0$ (dash-dotted curves). It can be seen that the microscopic potential leads to the same results like those in the case when the form b) of the WS potential with three parameters has been used. A general conclusion can be made that the spin-orbit interaction should not be neglected. In Figure 3 the comparison with the experimental data of our results for cross sections at various energies and using different models for the ^{6}He density is given.

It can be concluded that the LSSM is the most successful one in the description of the elastic scattering data. Using the LSSM it is no necessary at 41.66 MeV/N to renormalize the OP's. Also, for $E = 71$ MeV/N only the ReOP is renormalized

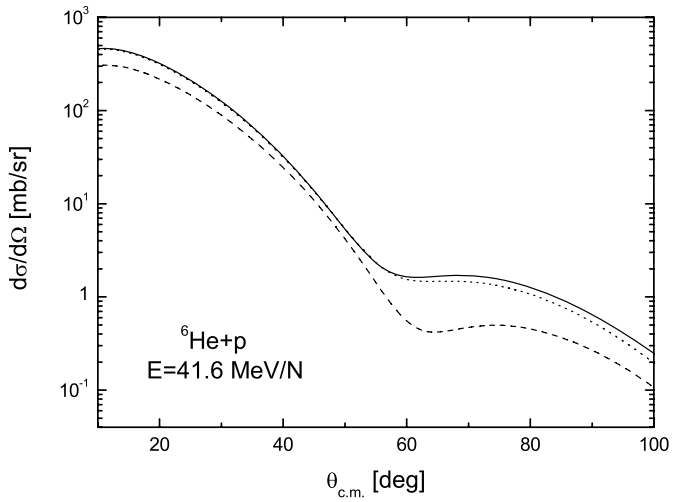

Figure 2. Elastic ^{6}He+p scattering cross section at energy $E = 41.6$ MeV/N calculated using the microscopic ReOP (V^F) in the spin-orbit term $(1/r)\mathrm{d}V^F/\mathrm{d}r$ (solid line) and also using the WS ReOP in $12.4(1/r)\mathrm{d}f^{WS}/\mathrm{d}r$ (dotted line). The dashed line shows calculations without the spin-orbit term. The LSSM density is taken for ^{6}He and the ImOP has the form of V^F.

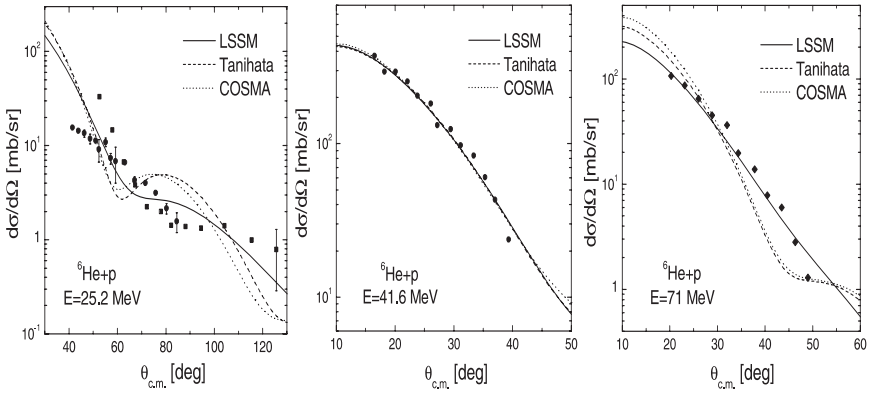

Figure 3. Elastic ^{6}He+p scattering cross sections at different energies calculated using $U_{opt} = N_R V^F + iN_I W^H$ for various values of the renormalization parameters N_R and N_I giving a reasonable agreement with the data (presented in Table 1). The used densities of ^{6}He are from LSSM (solid line), Tanihata (dashed line) and COSMA (dotted line). Experimental data for $= 25.2$ MeV/N are taken from [1–3], for $E = 41.6$ MeV/N from [6, 8] and for $E = 71$ MeV/N from [9, 10].

(see Table 1). Concerning comparison of cross sections at $E = 25.2$ MeV/N, the W^H turns out to be too deep, which is natural to be when considering potential at a high-energy scattering. Nevertheless, if we keep it as a microscopic OP with a form of U^B_{opt} (4) but decrease substantially the contribution of its imaginary part, a quite

Table 1. The optimal values of the renormalization parameters N_R and N_I obtained by fitting the experimental data for the elastic ^{6}He+p cross sections (see Figure 3). In the calculations $U_{opt} = N_R V^F + iN_I W^H$ and LSSM, Tanihata and COSMA densities for energies $E = 25.2$, 41.6, 71 MeV/N are used. The depths of the corresponding potentials (in MeV) are presented in the bottom part of the Table.

Energy	25.2	25.2	41.6	41.6	71	71
Renormalization parameter	N_R	N_I	N_R	N_I	N_R	N_I
LSSM	0.6	0.8	1.0	1.0	0.6	1.0
Tanihata	1.0	0.6	1.0	1.0	1.0	0.5
COSMA	1.0	0.6	1.0	1.0	0.8	1.0
Strength of potential	$N_R V^F(0)$	$N_I W^H(0)$	$N_R V^F(0)$	$N_I W^H(0)$	$N_R V^F(0)$	$N_I W^H(0)$
LSSM	18.86	87.02	26.22	77.20	11.01	53.09
Tanihata	30.82	39.15	25.54	46.31	17.56	15.92
COSMA	29.70	30.05	24.73	35.54	13.78	24.44

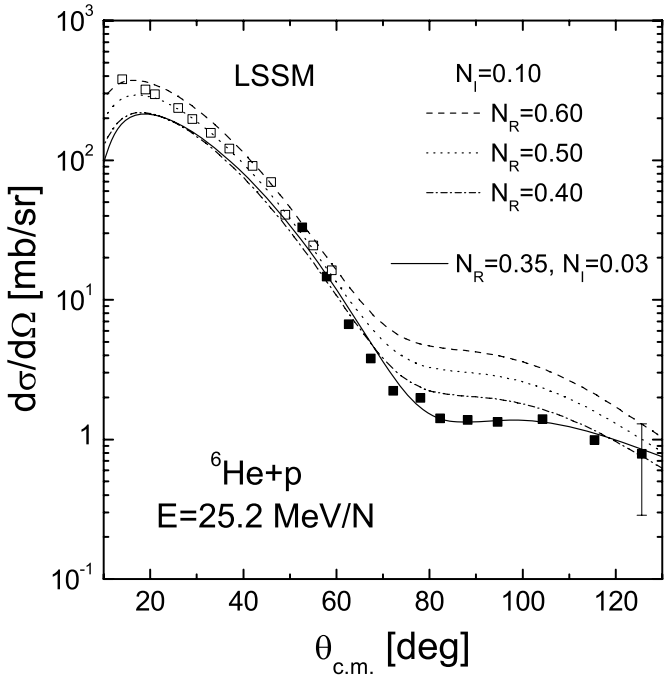

Figure 4. Elastic ^{6}He+p scattering cross sections for E=25.2 MeV/N calculated by using the LSSM density for ^{6}He. The curves present results for $U_{opt} = N_R V^F + iN_I W^H$ with different values of N_R (0.6 – dashed, 0.5 – dotted, 0.4 – dash-dotted) and fixed value of N_I=0.1. The solid curve is for N_R=0.35 and N_I=0.03. The experimental data are taken from [1–3].

reasonable agreement with the data can be achieved (see Figure 4). We note that such "shallow" potentials are typical for the phenomenological OP's.

Corresponding values σ_R of total reaction cross sections for all pairs N_R and N_I parameters (see Figures 3 and 4) are given on the Table 2 for $E = 25.2$ MeV/N. It is seen that σ_R mainly depends on the contribution of imaginary part of potential. The best fit ($N_R = 0.35$ and $N_I = 0.03$) gives the extremely small $\sigma_R = 57$ mb while for $N_I = 0.1$, σ_R is about 170 mb.

Unfortunately, the only experimental total reaction cross section of ^{6}He+p was measured at energy 700 MeV in [36, 37], it equals to about 160 mb. Of course, these energies are not comparable because the scattering mechanisms of low and higher energies are different. At $E = 25$ MeV, the reaction cross section is mainly determined by the ^{6}He structure while at $E = 700$ MeV, the most important is the effect of nuclear medium on a nucleon-nucleon interaction.

The experimental data on total reaction cross sections at low energies would be useful to understand a mechanism of the ^{6}He scattering and to improve the theo-

Table 2. The total reaction cross sections σ_R in dependence on the renormalization factors N_R and N_I of optical potential $U_{opt} = N_R V^F + iN_I W^H$ with the LSSM density of ^{6}He, for energy E=25.2 MeV/N.

N_R	0.6	0.6	0.5	0.4	0.35
N_I	0.8	0.1	0.1	0.1	0.03
$\sigma_R[mb]$	510	172	166	161	57

retical model (for example, by accounting for some other terms and effects that are neglected at this stage).

Methodical calculations have been performed in the present work as well. It is shown in Figure 5 the role of the density dependence of the NN forces. It is increased with the increase of the energy, but in our case this effect is small. Also, we performed calculations with and without accounting for the non-linearity that exists when the exchange part V^{EX} of the $V^F = V^D + V^{EX}$ is calculated. It is seen from Figure 6 that the role of the non-linearity is quite important and it should not be neglected. All curves in the previous figures have been calculated with an account for the spin-orbit interaction and for all the effects considered here.

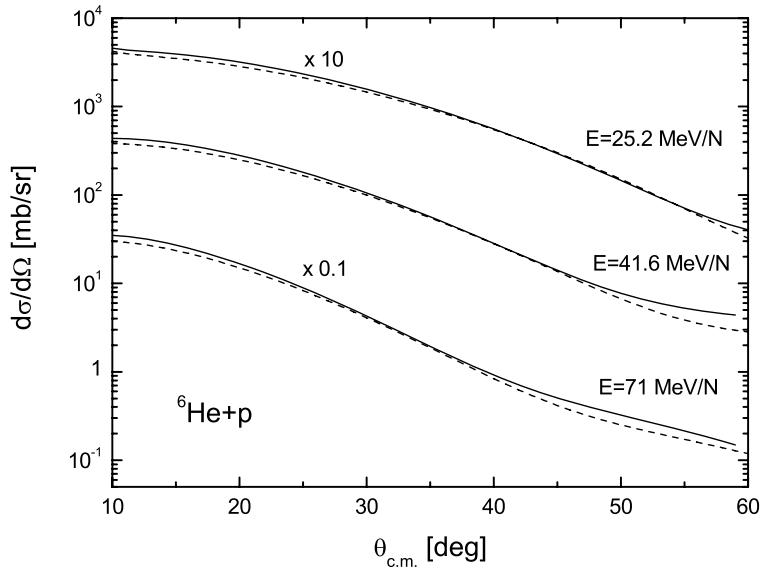

Figure 5. In-medium effect of the effective NN interaction on calculations of elastic ^{6}He+p scattering cross sections for different energies. The V^F is calculated with $F(\rho) = C[1 + \alpha \exp(-\beta\rho) - \gamma\rho]$ (solid lines) and with $F(\rho) = 1$ (dashed lines). The ImOP is calculated within the HEA W^H (see parameters of the calculations in [33]).

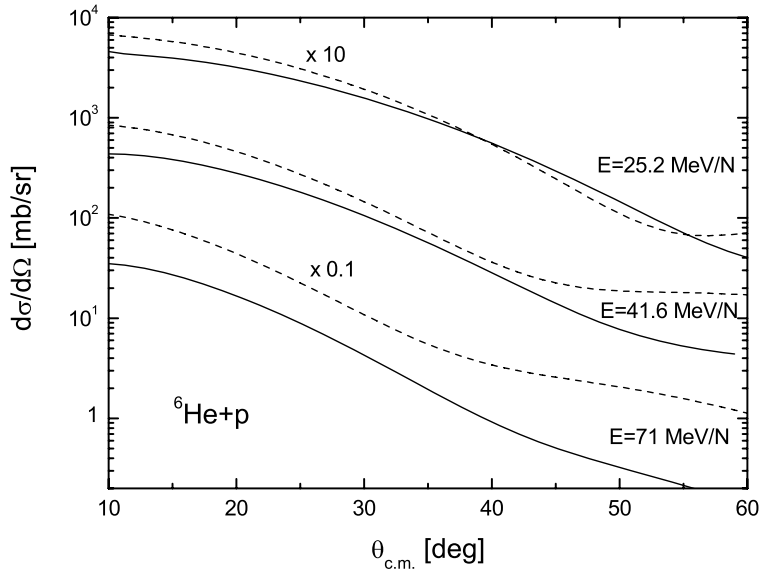

Figure 6. The non-linearity effect of elastic ^{6}He+p scattering cross section for different energies. The solid lines are the calculation results with the account for the non-linear effects in the ReOP, and by dashed lines are presented the results obtained without accounting for the non-linear effects. The LSSM density of ^{6}He is used. The imaginary part of OP is calculated within the HEA (W^H).

3 Conclusions

The main conclusion of the present work is that the application of the microscopic optical potentials with an imaginary part obtained within the HEA is justified in calculations of elastic scattering cross sections of the radioactive ^{6}He nuclei on protons at energies of 40–100 MeV/N. Best agreement with the data is achieved when the LSSM is used for calculations of the density of ^{6}He. In the case of $E = 41.2$ MeV/N it was no necessary to renormalize the depth of the OP, and at $E = 71$ MeV/N only one parameter $N_I^H = 0.6$ was introduced for the ReOP. In this way, for relatively small energies of a few tens of MeV/N it turns out to be more effective a procedure when one uses, instead of the HEA scattering amplitude within the Glauber-Sitenko theory [25, 26], the corresponding microscopic potential [27] and then solve numerically the Schroedinger equation. The point is that the HEA amplitude is based on the eikonal scattering phase in the form of the simple integral from the potential over the straight-line trajectory. However, when the energy decreases, in this amplitude one should integrate already over the real (curved) trajectory. Such integral can not be performed practically with the exception of the case of the trajectory in the Coulomb field of the potential of the form $1/r$. It turns out at the same time that the HEA potentials, including their imaginary part, are fully appropriate for interpretation of the data not only at high $E \gg U$ energies, but also at relatively small

$E > U$ energies, if these potentials are put directly in the Schroedinger equation. Actually it means that the distortion effects in the field of the potential with arbitrary form, including the microscopic one (obtained numerically) are strictly taken into account.

At energy $E = 25.2$ MeV/N the HEA potential does not work properly. It is necessary to decrease its strength in an order of magnitude for a correct description of the data. At processes of slow collisions the picture of the Glauber-Sitenko theory for the multiple nucleon scattering in the nucleus is not realized. Just opposite, instead of at least six collisions of the incident nucleon with nucleons of ^{6}He, that contribute the total nucleon-nucleus potential, already after the first collision the energy is transferred into the channel of a decay of the nucleus with an emission of two neutrons due to the low threshold of this channel. A weak absorption in the elastic channel (a "shallow" potential) corresponds to the process just mentioned and this is the reason for the necessity to renormalize strongly the microscopic ImOP.

Another peculiarity of the scattering mechanism is the substantial role of the non-linearity effects in the account for the exchange terms in the folding potential. These effects increase with the energy increase. They are included in the real part of OP and are still not accounted for in the ImOP that will be done.

Acknowledgments

The work is partly supported by the Program of cooperation between the INRNE (Sofia) and JINR (Dubna). The authors E.V.Z. and K.V.L. thank the Russian Foundation for Basic Research (Grant No.06-01-00228). A.N.A. and M.K.G. are grateful for support of the Bulgarian Science Fund under Contracts Nos. Φ–1416 and Φ–1501.

References

1. G.M. Ter-Akopian *et al.*, Phys. Lett. B **426**, 251 (1999); G.M. Ter-Akopian *et al.*, *in: Fundamental Issues in Elementary, Proceedings of the Symposium in honor and memory of Michael Danos, Bad Honnef, Germany, 2000*, edited by W. Greiner (E P Systema, Debrecen), 371 (2001).
2. R. Wolski *et al.*, Phys. Lett. B **467**, 8 (1999); S. Stepantsov *et al.*, Phys. Lett. B **542**, 35 (2002).
3. L. Giot *et al.*, Nucl. Phys. A **738**, 426 (2004).
4. R. Rusek K., K.W. Kemper, R. Wolski, Phys. Rev. C **64**, 044602 (2001).
5. V. Lapoux *et al.*, Phys. Lett. B **517**, 18 (2001).
6. M.D. Cortina-Gil *et al.*, Nucl. Phys. A **616**, 215c (1997).
7. A. Lagoyannis *et al.*, Phys. Lett. B **518**, 27 (2001).
8. M.D. Cortina-Gil *et al.*, Phys. Lett. B **371**, 14 (1996).
9. A.A. Korsheninnikov *et al.* Nucl. Phys. A **616**, 189c (1997).
10. A.A. Korsheninnikov *et al.*, Nucl. Phys. A **617**, 45 (1997).
11. L.L. Chulkov, C.A. Bertulani, A.A. Korsheninnikov,Nucl. Phys. A **587**, 291 (1995).

12. R. Crespo, J.A. Tostevin, R.C. Johnson, Phys. Rev. C **51**, 3283 (1995).
13. M.V. Zhukov *et al.*, Phys. Rep. **231**, 151 (1993).
14. M.V. Zhukov, A.A. Korsheninnikov, M.N. Smedberg, Phys. Rev. C **50**, R1 (1994).
15. M. Avrigeanu, G.S. Anagnostatos, A.N. Antonov, J. Giapitzakis, Phys. Rev. C **62**, 017001 (2000).
16. M. Avrigeanu, G.S. Anagnastatos, A.N. Antonov, V. Avrigeanu, Int. J. Mod. Phys. E **11**, 249 (2002).
17. M. Avrigeanu, A.N. Antonov, H. Lenske, I. Stetcu, Nucl. Phys. A **693**, 616 (2003).
18. G.R. Satchler, W.G. Love, Phys. Rep. **55**, 183 (1979); G.R. Satchler, *Direct Nuclear Reactions*, (Clarendon, Oxford, 1983).
19. D.T. Khoa, G.R. Satchler, Nucl. Phys. A **668**, 3 (2000).
20. O.M. Knyaz'kov, Particles and Nuclei **17**, No. 2, 165 (1986).
21. K.V. Lukyanov, Communication JINR **P11-2007-38**, Dubna (2007).
22. H. Feshbach, Ann. Phys, **5**, 357 (1958).
23. J.H. Sørensen, A. Winther, Nucl. Phys. A, **550**, 329 (1992).
24. G. Pollarolo, R.A. Broglia, A. Winther, Nucl. Phys. A **406**, 369 (1983).
25. R.J. Glauber, *Lectures in Theoretical Physics* (N.Y.: Interscience), 315 (1959).
26. A.G. Sitenko, Ukraine Fiz. J. **4**, 152 (1959).
27. V.K. Lukyanov, E.V. Zemlyanaya, K.V. Lukyanov, Phys. Atomic Nucl. **69**, No. 2, 240 (2006).
28. P. Shukla, Phys. Rev. C **67**, 054607 (2003).
29. S. Charagi, G. Gupta,Phys. Rev. C **41**, 1610 (1990).
30. P. Shukla, `ArXiv:nucl-th/0112039`.
31. I. Tanihata, Phys. Lett. B **289**, 261 (1992).
32. S. Karataglidis, P.J. Dortmans, K. Amos, C. Bennhold, Phys. Rev. C **61**, 024319 (2000).
33. K.V. Lukyanov, V.K. Lukyanov, E.V. Zemlyanaya, A.N. Antonov, M.K. Gaidarov, European Phys. J. A **33**, 389 (2007).
34. P.D. Kunz, E. Rost, *Computational Nuclear Physics* **2** (Eds: Langanke K. *et al.*, Springer Verlag), 88 (1993).
35. F.D. Becchetti Jr., G.W. Greenlees, Phys. Rev. **182**, 1190 (1969).
36. S.R. Neumaier *et al.*, Nucl. Phys. A **712**, 247 (2002).
37. G.D. Alkhazov *et al.*, Nucl. Phys. A **712**, 269 (2002).